Field Measurements of Flow Velocities in Propeller Jets

Irene Cantoni[1], Arne Van Der Hout[2(✉)], Erik Jan Houwing[3], Alfred Roubos[4], and Michel Ruijter[3]

[1] Civil Engineering and Geosciences, TUDelft, Delft, The Netherlands
[2] Deltares, Harbour, Coastal and Offshore Engineering, Delft, The Netherlands
Arne.vanderHout@deltares.nl
[3] Rijkswaterstaat, GPO, Utrecht, The Netherlands
[4] Port or Rotterdam Authority, Port Development, Rotterdam, The Netherlands

Abstract. Propellers of ships generate high velocities adjacent to quay walls, jetties and locks. Generally, a bottom protection is installed in order to prevent instability due to scour. Although design guidance exist, propeller-induced loads are far from fully understood and have predominantly been derived on the basis of model tests. The validation of the existing design methods is lacking, especially for specific types of bow thrusters. In this research, field measurements of flow velocities induced by a 4-channel bow thruster system against a vertical quay wall have been performed. Test results showed a flow characterized by low mean velocities and large fluctuations, with the extent of reflected flow limited to few meters from the quay wall and inflow beneath the suction points playing a role.

Keywords: Propeller jet · Bow thruster · Quay wall · Field measurement · Bed protection

1 Introduction

Use of transverse thrusters, such as bow thrusters, is common during berthing procedures. Bow thruster-induced wash can cause scour (Roubos, et al., 2014), creating therefore the need for a bottom protection. Due to the interaction between propeller, ship hull and lateral restrictions such as quay walls and sea bed, the flow pattern of the jet is quite complex and is characterized by turbulence and high flow velocities near the bed. An accurate understanding of the propeller-induced flow field is fundamental for engineers, in order to quantify scour and to design an adequate bed protection (Hamill and Kee, 2016).

While an unconfined jet has received attention from several studies, fewer research has been focused on the flow field induced by propellers when confinement elements, such as vertical quay walls or proximity to the sea bed, are present (Wei and Chiew, 2019). Most of the research on propeller induced flow has been based on Albertson *et al*., who used axial momentum theory to investigate the flow field of a plain-water jet (Albertson et al., 1950).

Y. Li et al. (Eds.): PIANC 2022, LNCE 264, pp. 82–100, 2023.
https://doi.org/10.1007/978-981-19-6138-0_8

General features of jets are: diffusion, mixing layers and a great amount of turbulence derived by decelerating flow (Verhagen, 2001). Using the results of Albertson et al., several others developed semi-empirical equations to describe the velocity field within a propeller jet, slightly modifying Albertson's equations. Fuehrer and Römisch (1987), Blaauw and van de Kaa (1978), Hoffmans and Verheij (2011) and Schmidt (2000) based their research on scale models, while Blokland (1996) conducted field measurements. Similar to the present research, Schmidt (2000) and Blokland (1996) investigated reflection of a propeller jet against a vertical quay wall, although they did consider a different type of (bow) thruster than investigated here. Based on Blaauw and van de Kaa, and Fuehrer and Römisch research, BAW (2010) and PIANC (2015) design guidelines have been developed.

In the most recent years, a series of studies identified discrepancies between expected theoretical values as computed using general design guidelines and scale or numerical models. Location of the maximum flow velocities and flow patterns were different than expected (Deltares, 2015). Another study, conducted in Hamburg by Danish Hydraulics (Köppen and Best, 2014), pointed the attention on current guidelines to be overly conservative. Furthermore, guidelines don't provide a clear indication with regard to the width of a bottom protection, which is often designed based on vessel characteristics instead on the extent of the flow velocities (PIANC, 2015).

This has created the need to increase knowledge about propeller jets, especially when reflecting from a vertical quay wall. Both the research community and industry show interest in the topic, with the final goal of achieving optimized bottom protection designs. This study is the result of a collaboration between Port of Rotterdam Authority, Rijkswaterstaat, Deltares, TU Delft, Rotterdam Municipality, Boskalis, Deme and CROW.

In November 2018, pilot measurements on this topic were conducted using a tug at the Antarcticakade, a quay wall for inland barges with a nautical water depth of approximately 7–9 m in the Port of Rotterdam (Deltares, 2018). During that measurement campaign, flow velocities in the propeller jet have been measured using a single upward looking Acoustic Doppler Current Profiler (ADCP). Measurement results indicated the applied set-up was adequate to measure propeller jets, being practical and applicable. Measurements carried out in the present research represent a follow-up study, using a similar test setup and taking place at the same location, with objective of obtaining a better understanding of the flow velocities that occur near the bed and to verify the applicability of design methods presently in use.

2 Field Measurements Methodology

For conducting the measurements, an inland motor vessel, MTS Vorstenbosch, was utilized (see Fig. 1, left panel). It was considered representative for ultimate design situations, since this inland vessel is the largest in the Netherlands. The quay wall at the Antarcticakade consists a sheet pile vertical quay wall, and it has a bed protection of a 20 m wide and 0.85 m thick layer of loose rocks 10–60 kg. For the first 10 m from the quay wall, the protection is penetrated with colloidal concrete (see Fig. 2).

Fig. 1. Measurement location with the Vorstenbosch (left); Schematic representation of a 4-channel bow thruster, illustrating the working principle of the system (Right, source: vethpropulsion.com).

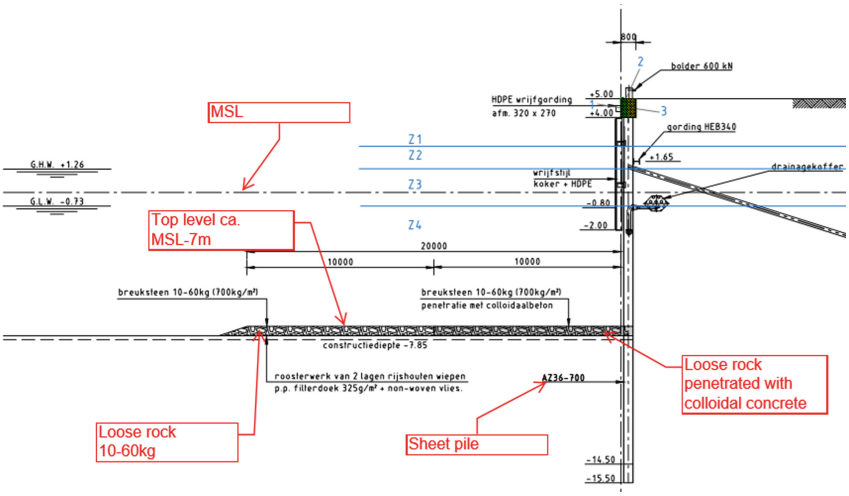

Fig. 2. Cross section of the Antarcticakade, with bottom protection characteristics highlighted.

The MTS Vorstenbosch is equipped with two 4-channel bow thruster systems (see Fig. 1, right panel). This vessel was selected, since for this type of thruster no clear design guidelines are yet available. Due to the shape of the bow of the vessel, the length of the thruster channel and the bow thruster inlet and outlet locations are different for each bow thruster. By applying different combinations of power for both bow-thrusters, it was therefore possible to test a wide variety of conditions. The characteristics of the vessel are listed in Table 1. For the most backward placed propeller (bow thruster 1), the wall clearance was equal to 4.23 times the propeller diameter Dt, and for the most forward propeller (bow thruster 2) the wall clearance was 2.32 times Dt.

Table 1. Characteristics of the Vorstenbosch

	Symbol	Parameter	Value
Ship	L	Length (m)	147.5
	B	Beam (m)	22.8
	D	Draught (m)	5.4
Veth Jet	Pt	Maximum power (kW)	618
4K-1400A	Dt	Propeller diameter (mm)	1420

To measure flow velocities, two Acoustic Doppler Current Profilers (ADCP) and two Acoustic Doppler Velocimeters (ADV) were installed (Nortek, 2017). While ADCPs measures an array of flow velocities, ADV sensors have a fairly small measurement volume (cylinder of 14 mm diameter and 14 mm height) with high sampling rate of 64 Hz. The ADCP measures the flow velocity in an array of cells by combining information of 4 acoustic beams, assuming a uniform flow within each measurement cell. The size of these measurement cells increases with increasing distance from the instrument. Due to the highly turbulent flow within a propeller jet, it was assessed that the assumption of uniform flow would not be met when the distance from the instrument would be too large. Therefore, here only the measurement results of the second cell of the ADCP are presented (located 0.5 m from sensor head), with a measurement volume that can be visualized as a pyramid trunk with a lateral area of 0.23 m base1 $\times$ 0. 41 m base2 $\times$ 0.20 m height (total approximate volume: 0.016 m^3) and a sampling rate of 8 Hz.

The instruments were mounted on a frame that was positioned on the sea bed, perpendicularly to the quay wall. One ADCP and one ADV were situated close to each other at the end of the frame near the quay, where maximum velocities are expected. One ADV was located in the middle of the frame, with the objective of being close to the bow thruster inlets and monitor the inflow. Finally, the last ADCP has been mounted at the external end of the frame, at $\sim$14 m from the quay wall. ADCPs were mounted horizontally, therefore looking underneath the ship's hull.

Three different ship positions have been considered. Firstly, the ship has been positioned with the axis of the bow thrusters symmetrical with respect to the measurement frame. Then, tests have been performed with the ship positioned 5 m ahead in respect to the first position, and 5 m behind it. Figure 3 (left panel) shows the three different adopted ship positions and their relative position to the measurement frame. A general reference system is adopted, with the positive x axis pointing perpendicularly away from the quay wall, y axis along the quay wall (positive towards the bow of the vessel), and z representing the vertical dimension in the water column (positive

upwards). To acquire insight in the spatial distribution of the flow, it is assumed that mean flow patterns are stationary and that the results of individual tests at different ship positions can be combined. Since moving the vessel was more efficient than installing additional instruments, this approach was adopted as a practical compromise. An illustration of the measurement points with respect to the vessel is depicted in Fig. 3 (right panel).

As a general measurement protocol, each bow-thruster was activated for 2 minutes for 4 applied power steps (25%, 50%, 75% and 100%), then both bow-thrusters were activated simultaneously also applying the same 4 power steps. The three tests were repeated for three different ship positions. Tests were then repeated both a low and high tide, to investigate influence of different keel clearances. To assess the influence of the changing water level, and identify eventual recirculation patterns, one test with a longer duration of 30 min was performed during the rising tide. In addition, one test where the ship is de-berthing was performed using both bow-thrusters at 100% of power, to allow a comparison of stationary tests with a realistic maneuver. Table 2 lists an overview of all performed tests.

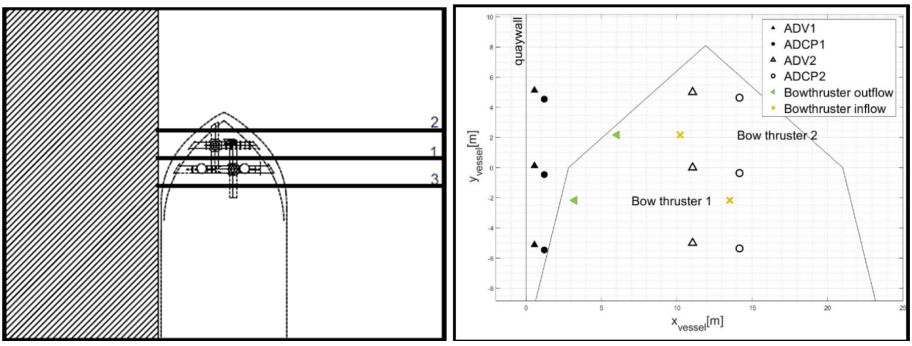

Fig. 3. The horizontal lines indicate the position of the frame on which the instrument where mounted with respect to vessel for the different considered ship positions (*left*); Illustration of the position of the instrument. ADVs are shown as triangles and cell 2 of ADCPs as circles. Inflow and outflow coordinates of both bow thrusters are illustrated, as well as a schematic outline of the ship (*right*).

Table 2. Measurement protocol for tests

Test	Subtest			Bow thruster	Ship position	Average keel clearance (m)
	Steps of applied power	Duration of each subtest (min)	Total duration of test (min)			
1	25%, 50%, 75%, 100%	2	8	1	1	1.03
2	25%, 50%, 75%, 100%	2	8	2		1.03
3	25%, 50%	2	4	Both		1.04
4	25%, 50%, 75%, 100%	2	8	2	2	1.06
5	25%, 50%, 75%, 100%	2	8	1		1.10
6	25%, 50%, 75%, 100%	2	8	Both		1.12
7	25%, 50%, 75%, 100%	2	8	1	3	1.30
8	25%, 50%, 75%, 100%	2	8	2		1.38
9	25%, 50%, 75%, 100%	2	8	Both		1.50
10	50%	30	30	Both	1	2.07
11	25%, 50%, 75%, 100%	2	8	1		2.57
12	25%, 50%, 75%, 100%	2	8	2		2.79
13	25%, 50%, 75%, 100%	2	8	Both		2.88
14	25%, 50%, 75%, 100%	2	8	1	2	2.82
15	25%, 50%, 75%, 100%	2	8	2		2.76
16	25%, 50%, 75%, 100%	2	8	Both		2.69
17	25%, 50%, 75%, 100%	2	8	1	3	2.58
18	25%, 50%, 75%, 100%	2	8	2		2.54
19	25%, 50%, 75%, 100%	2	8	Both		2.51
20	25%, 50%, 75%, 100%	2	8	1	1	1.33
21	25%, 50%, 75%, 100%	2	8	2		1.30
22	25%, 50%, 75%, 100%	2	8	Both		1.26
23	100%	7	7	Both	Moving	1.21

3 Test Results

3.1 General Flow Patterns

To investigate general flow patterns, the mean flow velocity and standard deviation for each step of applied power was calculated. Test 1, where bow thruster 1 was used at low tide for ship position 1, is taken as a base case; results are shown in Fig. 4 (left panel).

Observing the measured flow velocities for each instrument, it is possible to notice some general flow patterns. Instruments located near to the quay wall (ADCP1 and ADV1) recorded an increase in mean flow velocity with increase in applied power. Mean horizontal flow velocity appeared to be in the same order of magnitude for these two instruments, however the ADV recorded larger fluctuations. Also, the instrument located beneath the suction points (ADV2) showed an increase in mean flow velocity with an increase in applied power, but velocity magnitude was lower than recorded by the two instruments near the quay wall, and the trend seems different. The last instrument (ADCP2), located 14 m from the quay wall, recorded low mean flow velocities and the increase of applied power did not correspond to an increase in mean flow velocities.

These general observations are valid for most of the tests: mean flow velocities were usually in the order of magnitude of 1 m/s. The instruments near the quay wall presented a clear relation between an increase in applied power and an increase in velocities, whereas the instrument located beneath the suction points, despite recording an increase of velocity with increase of applied power, showed lower mean flow velocities. ADCP2 did not show a relation between use of bow thrusters and recorded velocities.

However, the data from the two instruments near the quay wall was not always consistent: the ADV often recorded higher mean flow velocities than the ADCP, and a larger variability, expressed by higher standard deviations. This behavior is especially evident in tests where the flow had more space to develop (larger keel and/or wall clearance). It is hypothesized that the relative low flow velocities measured by the ADCP is caused by the relatively large size of measurement cell compared to the turbulent structures present in the flow. However, this could not be confirmed during data processing and should be investigated further.

Concerning the spatial distribution of the flow: by assuming that placing the ship at a different position and combining individual test results is equivalent to have extra measurement points in the corresponding location, it is possible to gain an insight on the spatial distribution of the flow. This assumption was based on the uniformity of the measuring location. Test in different ship positions were performed with comparable water levels. A check conducted during post-processing gave confidence that the flow during the test was stationary enough to capture the small variations, as well as it did the absence of recirculation patterns during test 10. The only uncertainty on the validity of this assumption is represented by the variability of the sheet pile wall. Nonetheless, the results from the tests conducted with the ship located in position 2 and 3, consistently shown flow velocities significantly lower than the ones recorded for tests with the ship in position 1, giving a clear indication of the extent of the flow along the quay wall.

As observable in Fig. 4 (right panel), measurements do not show a clear return flow underneath the ship as there is a large variability in flow direction. Measurement points further away from the outlet do not seem to measure the reflected jet but show that the flow near the inflow point was directed towards the suction points of the bow thrusters. A comparison of flow direction recorded by the instrument located between the two suction points (ADV2), confirms that at this location ($\sim$10 m from the quay wall) the flow was dominated by the inflow and not by the reflected jet from the quay wall. This became particularly evident when comparing tests where different bow thrusters were used. Depending on which one is activated, the flow was directed towards the respective suction point (Fig. 5).

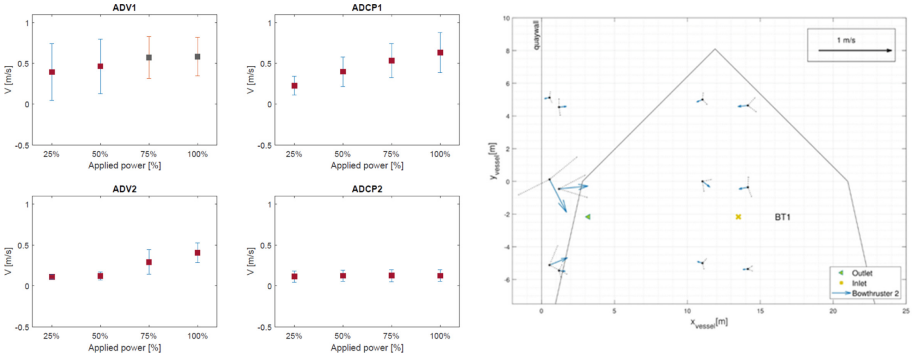

Fig. 4. Results from test 1 (use of bow thruster 1, ship position 1, low water). Horizontal mean velocity and standard deviation for each subtest are presented for each instrument. Non reliable data is colored in grey (*left*); Mean horizontal velocity magnitude and dominant direction for bow thruster 1 induced flow field at 50% of applied power. Tests 1, 5 and 7 (low water) have been combined. Dotted lines: range in direction, corresponding to $\pm$st. Dev of direction (*right*).

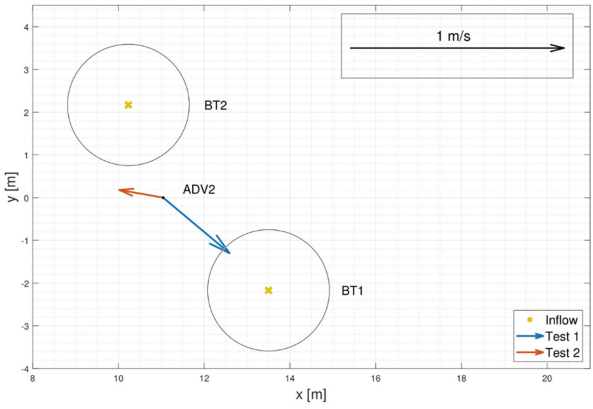

Fig. 5. Comparison of mean velocity and dominant direction measured by ADV2 for 100% of applied power in test 1 (bow thruster 1) and test 2 (bow thruster 2). Suction points of both bow thruster projections on the bed are shown.

3.2 Influence of Wall Clearance

To investigate impact of different wall clearances, the tests using one or the other bow thrusters were compared. The two bow thrusters differ in channel length, and hence in the resulting wall clearance. Wall clearances of the bow thrusters are, relative to the propeller diameter, respectively 2.32 D_t for bow thruster 1 and 4.23 D_t for bow thruster 2. For both bow thrusters however, also the relative position of the instruments with respect to the outlet was different. It was assumed that for this set-up, this difference was not relevant. Figure 6 shows that when low water tests are compared, no significant differences can be observed between the use of one or the other bow thruster, despite the asymmetric shape of the bow. For this condition, the influence of wall clearance seems small. When assessing the influence of under keel clearance however, the results are different for bow thruster 1 and bow thruster 2. This suggests that the impact of the under keel clearance is depending on the wall clearance and vice versa (Fig. 6).

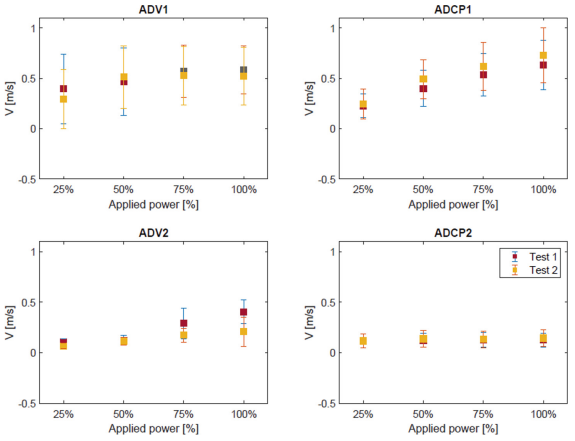

Fig. 6. Comparison of horizontal flow velocity mean magnitude and standard deviation for each step of applied power for test 1 (bow thruster 1) and test 2 (bow thruster 2), at low water.

3.3 Influence of Under Keel Clearance

Comparing the tests conducted at low or high tide, it is possible to observe the influence of under keel clearance on bed velocities. The results, as it can be observed in Fig. 7, vary depending on which bow thruster is used. Observing the data collected by ADV1, the use of bow thruster 1 seems to result in lower values of mean horizontal flow velocities with a larger under keel clearance. On the contrary, when bow thruster 2 is used, ADV1 records larger mean horizontal flow velocities with a larger under keel clearance, as well as an increase in turbulence.

This is though not reflected by measurements from ADCP1, which recorded similar velocities for both cases. It is also worth noting how, for bow thruster 2, the difference in mean horizontal flow velocity between low and large under keel clearance recorded

by ADV1 increased with the increase in applied power (Fig. 7, right). In contrast for bow thruster 1, the difference remained fairly constant (Fig. 7, left). From this result, it therefore appears that the influence of under keel clearance on the bed velocities also depends on wall clearance.

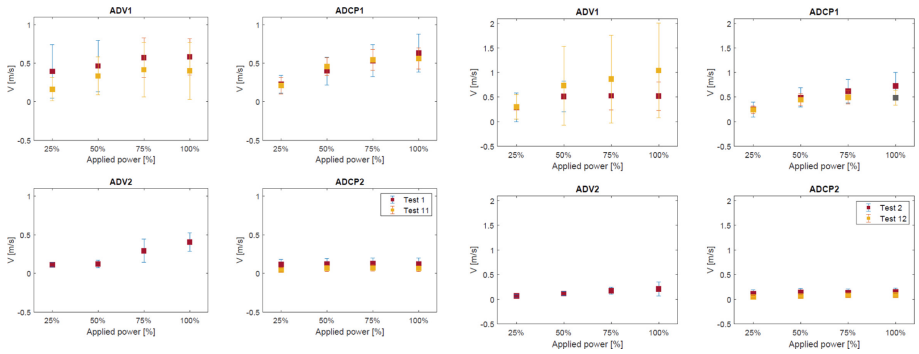

Fig. 7. Comparison for bow thruster 1 of horizontal mean flow velocity and standard deviation for each step of applied power for test 1 (low water) and test 11 (high water) (*left*); Same for bow thruster 2 for test 2 (low water) and test 12 (high water) (*right*).

3.4 Use of Multiple Bow Thrusters

Simultaneous use of the bow thrusters was also investigated during this research. Figure 8 (left panel) compares the results of tests 1, 2 and 3. In these tests, bow thruster 1, bow thruster 2 and both bow thrusters have been used during low tide. It seems that the use of both bow thruster simultaneously resulted in significantly higher flow velocities as could be expected. It should be noted that test 3 has been conducted only for the first two steps of applied power. This comparison is also possible for tests 11, 12 and 13, where respectively bow thruster 1, 2 and both bow thrusters simultaneously were used, but during high tide (Fig. 8, right panel). While tests 1, 2 and 3, presented above, were conducted at low water and with a fairly constant water depth, tests 11, 12 and 13 were carried out at high water and with larger variation in water level. There was, in fact, a difference of approximately 30 cm between water depth in test 11 and in test 13.

Figure 8 (right panel) shows that differences between use of bow thruster 1 and bow thruster 2 were more significant than the difference between the use bow thruster 2 or both bow thrusters at the same time. It is also worth noting the discrepancies in data recorded by the two instruments located near the quay wall (ADV1 and ADCP1), and the fact that velocities recorded by ADV1 during test 13 did not increase constantly with the increase in applied power, differently than in the other tests. The reason for this was unclear. Consequently, simultaneous use of both bow thrusters do not seem to lead to differences in mean flow velocities larger than the ones between the use of each bow thruster singularly for large keel clearances.

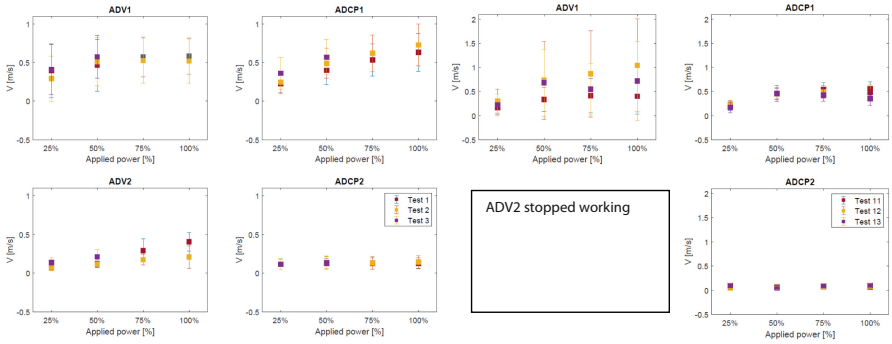

Fig. 8. Comparison of horizontal flow velocity mean magnitude and standard deviation for each step of applied power for test 1 (bow thruster 1) and test 2 (bow thruster 2), and test 3 (both bow thrusters) at low water (*left*); Same for test 11 (bow thruster 1) and test 12 (bow thruster 2), and test 13 (both bow thrusters) at high water (*right*).

4 Comparison with Guidelines

Results from field measurements were compared to the theoretical predictions using the formulae suggested by commonly used guidelines.

4.1 Maximum Velocities at the Bottom

The maximum velocities at the bottom have been estimated on the basis of both the Dutch and the German method suggested by PIANC. Equations suggested by the guidelines are based on the efflux velocity V_0, which depends on the power of the bow thruster P_t, water density ρ_w, and propeller diameter D_t as:

$$V_0 = 1.15\left(\frac{P_t}{\rho_w D_t^2}\right)^{0.33} \tag{1}$$

Furthermore, the maximum velocities V_{max}, which can be expected at the corner between the quay and the bed, can be calculated according to German method from:

$$V_{max} = a_L 1.9\, V_0\left(\frac{L}{D_p}\right) \tag{2}$$

where a_L is an empirical coefficient chosen based on wall and under keel clearance and L is the wall clearance. Following Dutch method, V_{max} is calculated using the following equations, with h_t the height of the thruster above the bed:

$$V_{max} = V_0 \frac{D_t}{h_t} \qquad for \frac{L}{h_t} < 1.8 \tag{3}$$

$$V_{max} = 2.8\, V_0 \frac{D_t}{L + h_t} \qquad for \frac{L}{h_t} > 1.8 \tag{4}$$

The data obtained from measurements are compared to the theoretical predictions in Fig. 9 (left and right panel) for both bow thrusters and respectively for a keel clearance of ~1 m, and ~2.7 m. This comparison shows that both formulae are generally conservative compared to the measured velocities, with the exception of data measured during use of bow thruster 2 at high water (test 12, see Fig. 9, right panel). Furthermore, it is possible to observe how sensitivity the methods are to variations in wall and under keel clearance. This could also be because some of the considered wall and under keel clearance ratio falls outside the range of values for which the formulae have been developed and validated.

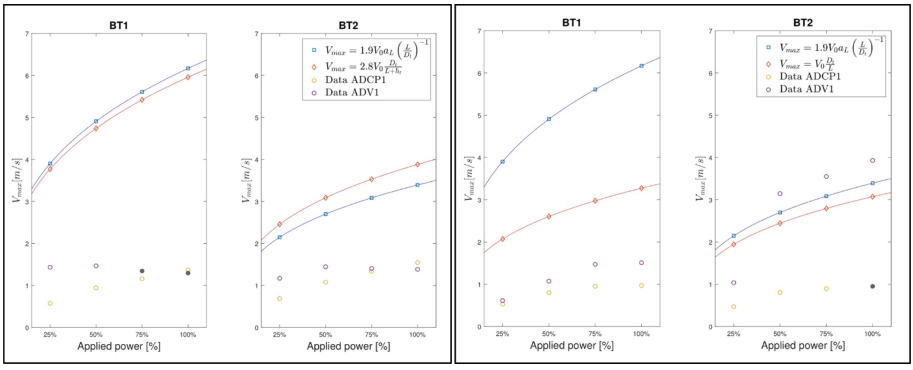

Fig. 9. Comparison between maximum velocities on the bed, as calculated with Dutch and German method, and measured maximum velocities from ADV1 and ADCP2 with a small UKC in Test 1 and Test 2 (*left*); Same for a larger UKC in Test 11 and Test 12 (*right*). Unreliable data (low correlation) depicted in grey.

4.2 Relative Turbulence Intensity

Relative turbulence intensity is a parameter that is often used to give an indication of turbulence level and can be calculated as $r = \frac{\sqrt{u'^2}}{\overline{u}}$, ratio between the root-mean-square of turbulent fluctuations u', and mean velocity $\overline{u}$. . Previous literature focused mainly on unrestricted flow; moreover, several methods (full scale measurements, scale models, analytical relations) were used. This resulted in a quite large typical range for relative turbulence intensity. Current guidelines indicate 0.25–0.4 as a typical range of values for r in propellers jet (PIANC, 2015). Figure 10 shows the data collected during the field measurements and shows that values are generally larger. This is mainly since the measured flow was characterized by low mean flow velocities and large fluctuations. The instruments near the quay wall record relative turbulence intensity levels even in the order of magnitude of 1.

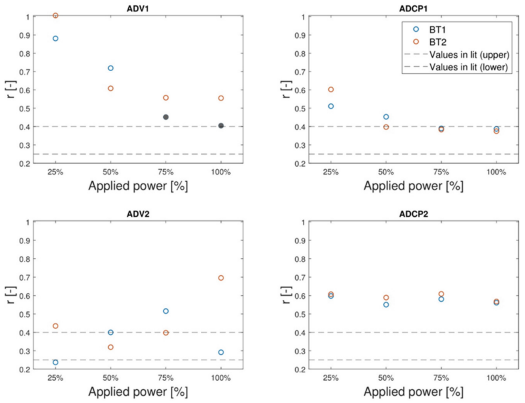

Fig. 10. Relative turbulence intensity measured by each instrument for each step of applied power. Comparison between bow thruster 1 (test 1) and bow thruster 2 (test 2). Unreliable data are depicted in grey. Reference lines indicate lower- and upper-bound values expected from literature.

4.3 Use of Multiple Propellers

According to literature, two approaches were adopted to take into account the use of multiple propellers: either linear superposition (PIANC, 2015) or proportionality to square root of number of propellers used (Schiereck, 2016). As observable from Fig. 11 both theories result to be generally conservative. Data collected during test 22 by the ADV is an exception (Fig. 11, right panel) and measurement results seem to be close to theoretical values obtained by multiplying theoretical velocities of one propeller by $\sqrt{2}$.

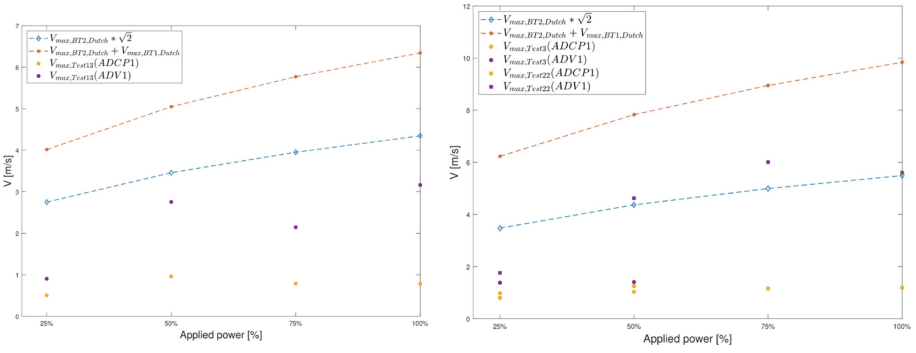

Fig. 11. Comparison of linear superposition theory and proportionality to sq. Root of n° of used propellers, with data from ADV1 and ADCP1 during test 13 (both bow thrusters, high water) (*left*). Same during test 3 and test 22 (both bow thrusters, low water) (*right*). Unreliable data in grey.

5 Discussion

5.1 Assessment of the Measurement Set-Up and Protocol

The measurement set-up used includes some limitations. Firstly, the efflux velocity of the thruster V_0 could not be measured directly with the used measurement setup. In the comparison of the measurement results with the design guidelines, the theoretical value of V_0 has been estimated based on Eq. (1) and the applied power as read from the instrument panel in the ship cabin. It is possible however that the actual efflux velocity in the field tests was lower than this theoretical value and that part of the conservatism shown in Section 4 is originating from the uncertainty in actual efflux velocity. It is therefore advised to measure V_0 directly in future research to verify the validity of Eq. (1) for these types of 4-channel bow thrusters.

Secondly, the limited amount of measuring points and the low spatial resolution result in a fragmented knowledge of the spatial patterns of the flow. ADCPs should have provided more insight on the extent of the reflected flow, but due to the high level of turbulence caused by the reflected jet, the cells more distant from the instrument were considered not reliable due to their relatively large measurement volume. Furthermore, in some tests there is a clear discrepancy between the two instruments placed near the quay wall. Despite their vicinity, ADV1 and ADCP1 are often showing different results. Namely, the ADV records higher mean flow velocities and larger fluctuations than the ADCP. Moreover, velocities corresponding to pressure fluctuations recorded by the ADCP appear to be larger than the recorded flow velocities. This could raise the suspicion that the ADCP, that averages the flow over measuring volume, it is not able to capture the turbulent flow caused by the bow thrusters. Therefore, we consider the flow measured by the ADVs to be more reliable, although the ACDP data can still valuable in a qualitative way, e.g. for relative comparison between different tests and showing trends in the data.

Despite the discrepancies and uncertainties above mentioned, the used measurement set-up was able to clearly determine three different zones in the bow thrusters-induced flow on the bed. These zones fit in the framework identified by Schmidt and we adapted it for 4-channel type bow thrusters. Figure 12 illustrates these zones of the flow induced by the reflection of bow thrusters against a vertical quay wall.

- Outflow zone (zone 1): differently than Schmidt, who distinguished an establishment flow zone and an established flow zone, for these tests only an outflow zone was identified. This is chosen on basis of the comparison between tests where bow thruster 1 was used (flow should have not been developed yet when it impinges the quay wall) and bow thruster 2 (flow should have been developed at the impingement). Since no major differences were observed, only one zone is assumed for the considered wall clearances;
- Impingement zone (zone 2) and spread along the quay wall (zone 3) were the zones identified by Schmidt in his experiments. During the present study, the focus was on the near bed velocities. Therefore, these zones haven't been investigated;
- A reflection zone (zone 4), where the flow is characterized by the highest recorded velocities and presents a clear relation with the use of bow thrusters;

- An inflow zone (zone 5), where the flow presents lower velocities than in the reflection zone, but still correlates to the use of bow thrusters. The flow is directed towards the 4-channel system suction point(s);
- A zone (zone 6) where the use of the bow thrusters is not noticed by the instruments anymore. At 14 m from the quay wall, flow velocities are low and there is not an increase in velocity following the increase of applied power from the bow thrusters.

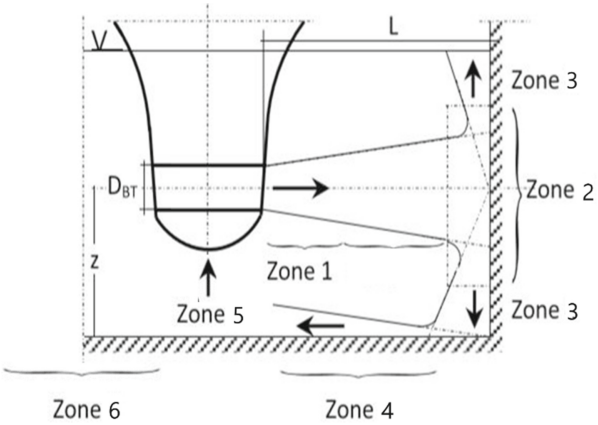

Fig. 12. Zones of reflected jet identified by the tests analyzed in this paper. Adapted by the authors from Schmidt (2000).

Furthermore, the used set-up confirmed the two assumptions that were made during testing. The first assumption was that activating the bow thrusters with the ship moored at the quay would be representative of realistic mooring operations. To test this hypothesis, a test was performed with the ship de-berthing, both bow thrusters activated at 100% of power. Results from this test show that mean velocities of the dynamic situation are comparable with the ones from the static one (see Fig. 13). Since the guidelines provide calculations for the mean velocity, the focus on the dynamic test was on the moving mean. These values were comparable with the ones in the static tests. The higher instantaneous velocities recorded by ADV1 shown in Fig. 13 may be partly influenced by measurement errors and should be investigated further. Stationarity checks conducted on the static tests ensured that the mean over each subtest is representative. Therefore, the results from tests 1–9 and 11–22 are considered representative for a realistic berthing or de-berthing situation.

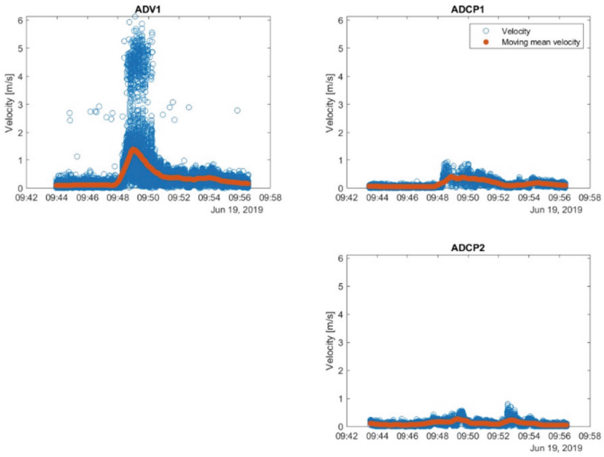

Fig. 13. Time series of recorded horizontal flow velocities during test 23 (de-berthing maneuver, both bow thrusters activated at maximum power). Both instantaneous and moving mean over 1 min are shown.

5.2 Contextualization in the Theoretical Framework

From comparison with Dutch and German calculation methods of near-bed flow velocities recommended by PIANC guidelines, data collected in this study identified the guidelines as conservative in most cases, especially the ones were the maximum absolute velocities were recorded and are, therefore, determinant for design. On the other side, data recorded by ADV1 in some tests, namely test 12 and 22, resulted in maximum velocities at the bottom slightly larger than the expected ones. Both in test 12 and test 22, bow thruster 2 was used: in test 12 on its own, in test 22 simultaneously with bow thruster 1. Bow thruster 2 is characterized by a larger wall clearance, equal to 4.23 D_t, while bow thruster 1 is located at 2.32 D_t from the quay wall. Most of the research upon which the guidelines have been based considered situations where the flow was less restricted than in the case presented in the present study: (Blaauw and Van de Kaa, 1978) conducted physical scale modelling for ducted and non-ducted propellers, measuring the velocities as the ship was moving in relatively unrestricted waters. (Schmidt, 2000) studied propeller jets against a quay wall in a stationary situation, evaluating different wall and keel clearances. Wall clearance studied by Schmidt were between 7.3- and 4-times D_t, while height of the thruster in the water column was either 2.2- or 2.4-times D_t. In the present study, height of the bow thruster changed more gradually within the tests, covering values between 1.21 D_t and 2.45 D_t. The results of the present study for the situation with a height of the bow thruster of 2.45 D_t and a wall clearance of 4.23 D_t fall within the range explored in Schmidt experiments. As Fig. 9 illustrates, maximum velocities recorded by the ADV present a similar trend to the one forecasted following the German method. However, the maximum velocities recorded by the ADV were slightly larger than expected. For the test with an under keel and wall clearance outside the range taken into account by the

studies upon which the guidelines were drafted, the results showed the guidelines to be over conservative.

In combination with the aforementioned smaller wall clearances associated with the bow thruster system, the results of the present study show how the flow develops in a more restricted environment compared to previous studies and shows that for these conditions the design guidelines are conservative. Already a physical scale model research performed by Deltares (2015) found that formulae in literature being generally conservative for small wall clearances, with the exception of larger distances between quay wall and ship (9.5 D_t). Blokland (1996) as well, using field measurements, found higher flow velocities than expected from calculations for wall clearances between 3.2 D_t and 16 D_t.

These results support the hypothesis that currently generally used guidelines do not reflect influence of wall and keel clearance accurately enough for restricted situations, which are outside the range of tested conditions on which the theoretical formulations used in design guidelines are based. These conclusions are relevant, since the situation of small wall clearance considered in the present field measurements is representative for most inland vessels, which are usually characterized by a blunt hull shape that results in a small distance between the wall and the bow thruster's outlet.

5.3 Impact on Bottom Protection Design

When using measured flow velocities in the commonly used stability formulae to determine a suitable rock size required for bed protection, results vary greatly according to which tests are chosen as representative for design conditions. Concerning stability formulas such as Izbash and Pilarczyk, one should consider that these formulations have not been specifically developed for propeller jets. For propeller-jet induced damage, and stability in general, turbulence has been previously identified as a mechanism which might be even more important than mean flow velocity, for instance by Verhagen (2001) and Hofland (2005). As observed in Paragraph 4, low values of mean flow velocities and high relative turbulence intensities were present near the bed. The resulting calculations of rock stability for these conditions suggested that some damage would occur at the Antarcticakade for the most severe conditions. However, surveys conducted after the measurements did show an absence of damage (no displaced rocks) and also the instruments did not show any signs of impact due to moving loose material. This leads to think that a more precise representation of the physical phenomena should be sought.

6 Conclusions

From the measurements conducted at the Antarcticakade quay wall, bow thruster-induced flow on the bed seems to be characterized by fairly low mean flow velocities in combination with a high relative turbulence level. In contrast to research that was previously conducted, no clear return flow underneath the vessel was observed. The extent of the reflected flow from the quay wall seemed to be limited to a few meters. In addition, the flow pattern below the vessels seems to be largely influenced by the

suction points of the 4-channel bow thruster system. Furthermore, the measured flow velocities for small wall and under keel clearances showed to be much lower than predicted by methods that are presently used in the design of bottom protections. For larger keel and wall clearances, a better match with general design guidelines was found, but the maximum velocities were slightly larger than expected. Consequently, the design guidelines for bottom protection seem to be conservative for berths facilitating inland vessels in situations with small under keel clearances (approximately < 2 D_t) and small wall clearances (approximately < 4 D_t). It is however important to note how more restricted situations are more relevant for design, since they cause the largest absolute flow velocities. These results are in agreement with previous scale model tests conducted by Deltares (2015). It is highly recommended that additional tests be performed to derive more insight into the relation between the flow velocities near quay walls and small under keel and wall clearances.

Acknowledgements. On behalf of the Delft University of Technology, Deltares, Port of Rotterdam, and Rijkswaterstaat the authors of this paper would like to thank all companies involved for their support, funding and hospitality. In particular, VT and Shell are gratefully acknowledged for their support and for providing a fully laden Vorstenbosch for this test.

References

Albertson ML, Dai YB, Jensen RA, Rouse H (1950) Diffusion of submerged jets. Trans. Am. Soc. Civ. Eng. 115(1):639–664. https://doi.org/10.1061/TACEAT.0006302

BAW: Principles for the design of bank and bottom protection for inland waterways. Code of Practice, Karlsruhe, March 2011, ISSN 2192-9807 (2010)

Blaauw HG, Van de Kaa EJ (1978) Erosion of bottom and sloping banks caused by the screw race of manoeuvring ships. In: 7th International Harbour Congress, May 22–26, 1978, Antwerp

Blokland T (1996) Schroefstraal Tegen Kademuur - Stroomsnelheid en Erosie Meeting (in Dutch), Gemeentewerken Rotterdam, Project Delta 2000-8

Deltares (2015) Propeller jets. Knowledge Gap 7 - Reflection of Transverse Jets by Vertical Quay Walls. Ref: 1210140-000-HYE-0008. 20 Nov 2015

Deltares (2018) Veldmetingen schroefstraalbelastingen (memo in Dutch), project number 11202175. 21 Dec 2018

Fuehrer M, Römisch K (1987) Propeller jet erosion and stability criteria for bottom protection of various constructions. PIANC Bullettin No. 58

Hamill G, Kee C (2016) Predicting axial velocity profiles within a diffusing marine propeller jet. Ocean Eng. 124:104–112

Hoffmans G, Verheij H (2011) Jet scour. Inst. Civ. Eng. Proc. Marit. Eng. 164(4):185–193. https://doi.org/10.1680/maen.2011.164.4.185

Hofland B (2005) Rock and Roll - Turbulence-induced damage to granular bed protection. PhD dissertation, TU Delft

Köppen J, Best J (2014) Messung von Schiffsinduzierten Belastungen auf das Bubendey Ufer Naturmessungen von Uferbelastungen. DHI

Nortek (2017) The Comprehensive Manual. Nortek

PIANC (2015) Report No. 180. Guidelines for protecting berthing structures from scour caused by ships

Roubos A, Blokland T, Van der Plas T (2014) Field Tests Propeller Scour Along Quay Wall. PIANC World Congress San Francisco, USA

Schiereck GJ (2016) Introduction to Bed, Bank and Shore Protection. Delft Academic Press/VSSD, Delft

Schmidt E (2000) Belastungen Durch Bugstrahlruder. Dresdner Wasserbauliche. Mitteilungen 18, Technische Universität Dresden, Institut für Wasserbau und Technische Hydromechanik, pp. 145–157. https://hdl.handle.net/20.500.11970/104017

Verhagen HJ (2001) Bowthrusters and the stability of a riprap revetment. https://www.researchgate.net/publication/238606205

Wei M, Chiew YM (2019) Impingement of propeller jet on a vertical quay wall. Ocean Eng. 183:73–86